

DESIGN, FABRICATION AND OPERATION OF REMOTELY CONTROLLED AIRSHIPS IN INDIA

Amol C. Gawale*, Amool A. Raina*, Rajkumar S. Pant*, Yogendra P. Jahagirdar**
 *Indian Institute of Technology Bombay, India ** Research Institute for Model
 Aeronautics, Ahmednagar, India

Keywords: *Remotely Controlled Airships, LTA vehicles*

Abstract

This paper describes shares the experiences gained by the authors in design, fabrication and testing of remotely controlled (RC) airships in India. A brief description of a methodology for sizing and baseline design calculations of an RC airship meeting some user specified requirements is presented. The section on design provides details of the standard envelope profiles for RC airships, types of materials use for envelope and fins and their properties, basic buoyancy and aerodynamic calculations, followed by stabilizer and fin sizing, and description of the propulsion system. The section on fabrication describes the Radio Frequency (RF) sealing method for realizing the envelope and fins, and discusses important issues related to the system integration and testing. Relevant details of two RC airships developed in India are presented, to illustrate the application of the methodology, and also to highlight some of the abovementioned issues.

Nomenclature

BM	=	bending moment
C _p	=	pressure coefficient
CFD	=	Computational Fluid Dynamics
D	=	maximum diameter
FRP	=	fiber reinforced plastic
h	=	height
g	=	acceleration due to gravity
ISA	=	international standard atmosphere
l/d	=	Length to diameter ratio
L	=	Load per unit length
LTA	=	Lighter than Air
r	=	radius
t	=	thickness of the fabric

V	=	Velocity
α	=	angle of attack
β	=	angle of sideslip
ρ	=	density
Δ	=	differential

Subscripts

a	=	air
aero	=	aerodynamic
he	=	Helium
hoop	=	hoop stress
int	=	internal
long	=	longitudinal stress
max	=	maximum
tot	=	total
∞	=	free-stream conditions

1 Introduction

Any application that requires a stable, low-cost, long endurance platform having low level of vibration, noise, and vehicle induced wind-disturbances is a potential candidate for employing airships. Airships can be utilized as a platform for mounting sensors for scientific experimentations such as collecting air or gas samples, measurement of local wind profiles, and solar irradiation, and agricultural applications such as spraying insecticides. A remotely controlled (RC) airship is perhaps much more suitable than a remotely controlled aircraft for some specific missions, such as prolonged aerial observation of any activity happening on the ground, (e.g., aerial coverage of sporting events, or security patrolling), long endurance loiter for product promotion, or precise dropping of payload (e.g., showering of flowers or confetti during religious functions or

inauguration/closing ceremonies). The design, fabrication and operation of RC airships, however, pose many challenges. The aim of this paper is to highlight these challenges and suggests ways and means to overcome them, based on the experience gained by the authors over the last few years.

1.1 Micro and Mini airships

A Program on Airship Design & Development (PADD) was launched at IIT Bombay, India in 2001[1]. The aim of this project was to develop indigenous expertise in airship technology. A methodology [2] for sizing and design of manned airships was developed as part of this project, and used for conceptual design and sizing of two manned airships viz., the Demo and PaxCargo. This methodology has been subsequently modified for design of RC airships, and is explained in this paper.

The PADD team developed an RC airship viz., *Micro*, (with an envelope volume of 6.82 m³) mainly to obtain a first hand exposure to issues related to airship design, fabrication and operation. This airship also acted as flying platform for flight demonstrations, and also generation of airship design data and experimentation. This activity was seamlessly integrated with an ongoing Aircraft Design Laboratory course for the undergraduate students of Aerospace Engineering Department. By participating in this activity, the students obtained a flavor of being a part of a design team and being involved in the development of an aerial vehicle right from conceptualization to the realization.

The design requirements specified for the *Micro* airship were very modest; it was required to have a payload capacity of 1.0 kg, while operating at a maximum speed of 30 kmph for 20 minutes, using an existing OSMG1415 IC engine, developing 0.41 BHP with a displacement of 2.49 cc. Due to constraints on storage space, it was required to be less than 5.00 m in length.

Subsequent to the successful development and flight demonstrations of *Micro* airship, the PADD team was invited by the government of

India to showcase their technology to the scientific community of India at a national science congress, and the PADD team developed the *Mini* airship for this purpose, which had an envelope volume of 8.64 m³, resulting in a payload capacity of 3.0 kg, and hence was capable of carrying out various missions, such as aerial surveillance. This airship was subsequently demonstrated at several other places. Further details of PADD and these two airships are available in [1].

2 Methodology for RC Airship Design

An RC airship can broadly be divided into the five main components, viz., Gondola, Propulsion system, Stabilizer and Fins, Remote Control system, and Envelope.

The methodology arrives at the sizing and layout of an RC airship based on the user specified performance and operational requirements. Some activities related to the design of RC airships are quite similar to that of RC aircraft, for instance the gondola, which is quite similar to that of the fuselage of a low speed RC aircraft. But there are some differences and additional options available while designing other components. For instance, the propulsion system of RC airships can be similar to RC aircraft, i.e., provision of thrust by propellers driven either by DC motors with onboard batteries or the IC engines. However, a thrust vectoring system is usually employed in RC airships to enhance its performance capabilities and controllability. The stabilizer and fins are sized keeping in mind the stability and control requirements, respectively; however, the dynamics of an airship are quite different from that of an aircraft, so the same sizing formulae and procedures cannot be used. Further, a yaw-motor is generally fitted in the stabilizer if the size of the fins is found to be insufficient to provide the required turn rates. The envelope of an RC airship has a similar function as the wing of an aircraft, i.e., providing the lifting force to overcome gravity; however, it is quite different in shape and size, mainly due to the radically different mechanism for generating the lift force.

Key issues related to the design of various components of airships are outlined in the subsections that follow.

2.1 Envelope Design

The first and foremost issue related to envelope design is its shape, which has to meet many conflicting requirements. The shape should result in large volume but low surface area, since the lift producing capacity of an airship envelope is directly proportional to its volume, and its weight is proportional to the surface area. If this was the only consideration, the best shape would have been spherical; however, such a shape would result in large drag, and hence lead to a much more powerful (and hence heavier) propulsion system. Further,

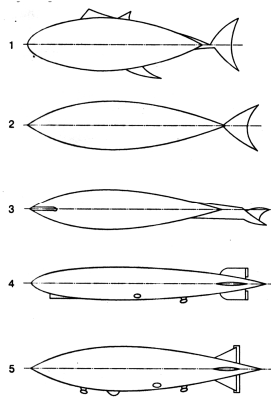


Fig. 1 Envelope profiles of Fish & airships 1- Tunny, 2- Tumak (Cuffy), 3-Whale, 4-Zeppelin, 5- R101

the stability and control requirements also drive the shape to be slender, resulting in larger moment arm for the stabilizers and fins and hence reduction in their sizes. It is not surprising that envelope shapes for airships are quite similar to that of fish, as shown in Fig. 1 [4]. Table 1 shows the comparative analysis of the key features of various shapes of fish and airships.

The airships that were used in the pre World War-II period had a very high slenderness ratio of the order of 10-11 which was subsequently reduced to 6-7 [4]. However, CFD analyses [6, 7], and an analytical study [8], have indicated that the slenderness ratio of envelopes should be between 3 and 5. Issues related to envelope shape optimization from

multidisciplinary considerations have been elaborated in an earlier study [3].

Table 1. Comparison between shapes of fish bodies and airships [4]

DESCRIPTION	SLENDERNESS RATIO	POSITION OF MAX DIA FROM NOSE
TUNNY	3.55	0.43
TUMAK	4.05	0.44
WHALE	4.60	0.36
ZEPPELIN	7.74	0.37
R-101	5.50	0.40
GNVR	3.05	0.41

Some standard shapes for airship envelopes have also been suggested in literature, such as the double ellipsoid NPL shape [5], and GNVR shape shown in Fig. 2, which has been used in India for design of aerostats.

The GNVR shape consists of three standard sections, and its entire geometry is analytically parameterized in terms of its max diameter D, as seen in Fig. 2.

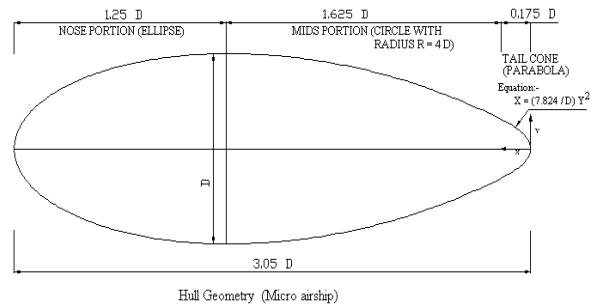


Fig. 2 Geometry of the GNVR Shape

For the *Micro* airship, the GNVR shape was chosen for the envelope since it offered a shape with considerably low drag coefficient and resulted in the smallest envelope surface area, while meeting the constraint on its length. However, no such constraint was present while design of the *Mini* airship, hence a double ellipsoidal shape was chosen.

2.2 Envelope Construction

Once the envelope shape is frozen, the detailing of other components can be carried out. The envelope group is further divided into components namely main envelope body

ballonet(s), catenary curtains, and load carrying patches, as shown in Fig 3.

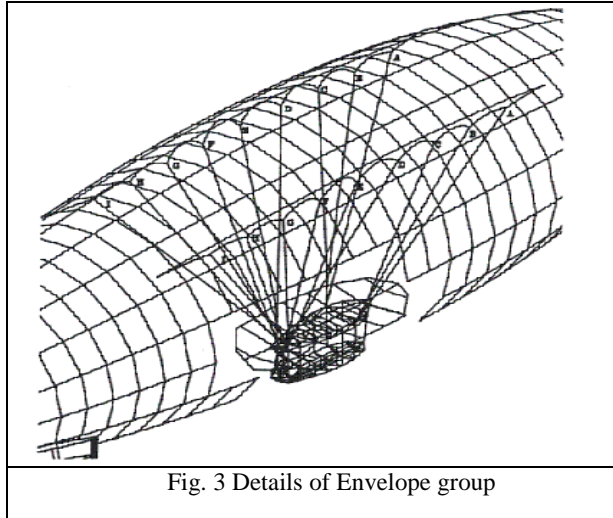


Fig. 3 Details of Envelope group

The envelope is usually constructed by joining smaller strips of fabrics as shown in Fig 4.

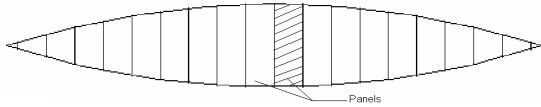


Fig. 4 A typical gore, showing panels

Each such piece is called a panel and a set of panels when joined together is called a gore. The number of gores and panels per gore is very critical from the envelope design point of view.

Three methods for approximating the shape of the envelope using flat patterns are generally available, viz., Gore, Zone and Compound Method [9].

The Gore method actually produces a shape with polygonal cross sections and true longitudinal curves. For the inflated envelope to be truly curved in all planes, all meridional path lengths must be equal and hence longitudinal threads in the gore center are more highly (e.g., Kevlar), this may introduce undesirable stress concentration. It is also possible to have unloaded and wrinkled seams along the gore edge [9]. loaded more than the threads at the edges. For an envelope material very high modulus (e.g., Kevlar), this may introduce undesirable stress concentration. It is also

possible to have unloaded and wrinkled seams along the gore edge [9].

Based on the type of approximation chosen, the direction of wrinkle formation can easily be determined. The actual wrinkle formation depends on the number of gores and breakup of gores into panels, and the elasticity of the envelope material.

As far as an airship is concerned, the wrinkles perpendicular to flight direction result in larger drag, while those parallel to the directions of flight are quite harmless. A comparison of the three methods of approximation is shown in the Table 2.

It was observed that due to multiple layers of fabric, the stiffness increases which results in lesser elongation at the seam compared to central part of the panel. This results in a wavy envelope surface. This waviness can lead to higher drag under certain conditions. Hence special attention needs to be given to this during fabrication. For the *Micro* and *Mini* airships, the Gore method was employed due to its small size and ease in fabrication.

2.2 Preliminary Structural Design of Envelope

In order to optimum fabric thickness, the various forces acting on the envelope are to be calculated. Envelope fabric thickness is determined by the circumferential and longitudinal stresses acting on it.

2.2.1 Circumferential Unit Stress

Circumferential Stress σ_{hoop} is often referred to as hoop stress and is used for calculating the maximum stress acting at the maximum diameter of an envelope.

$$\sigma_{hoop} = \frac{\Delta P_{int} \cdot 2r}{2t} = \frac{\Delta P_{int} \cdot r}{t} \quad (1)$$

Thus the load due to hoop stress per unit width

L_{hoop} is

$$L_{hoop} = \sigma_{hoop} \cdot t = \Delta P_{int} \cdot r \quad (2)$$

2.2.2 Longitudinal Unit Stress

Longitudinal Stress is used for checking the buckling parameters to ensure that the airship

fabric is always taut and wrinkles do not occur. Longitudinal stresses occur mainly due to two factors, viz., internal pressure and bending moment. Stress and unit load due to internal pressure can be estimated using Eq. 3 and 4, while the corresponding quantities due bending moment can be estimated using Eqn. 5 and 6, respectively.

$$\sigma_{long} = \pm \frac{BM \cdot r}{\pi r^3 t} \quad (3)$$

Thus the load due to longitudinal stress per unit width L_{long} is

$$L_{long} = \sigma_{long} \cdot t = \pm \frac{BM}{\pi r^2} \quad (4)$$

Eq. (5) refers to the total unit load acting in the longitudinal direction. Thus the load due to longitudinal stress per unit width L_{tot} is

$$L_{tot} = \Delta P_{int} \cdot r \pm \frac{BM}{\pi r^2} \quad (5)$$

2.3 Air flow around Envelope and Pressure Distribution at $\alpha = 0, \beta = 0$

Fig 5 shows the air flow around an envelope when angle of attack and angle of yaw are zero. Velocity goes on decreasing in front of the envelope and reaches a value of zero ($V = 0$) at the forward most point on envelope.

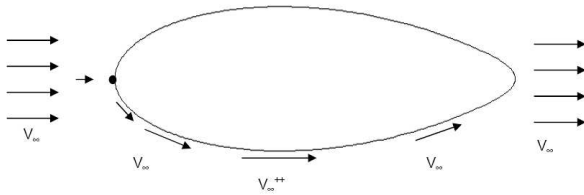


Fig. 5 Air flow around the envelope

As the flow continues around the envelope, the velocity goes on increasing and becomes equal to V_∞ and then, somewhere near the maximum diameter, reaches a maximum, which is much larger than V_∞ , so indicated as V_∞ . As the flow further moves ahead around the envelope, the velocity goes on decreasing and reaches theoretical value of zero at the rearmost point of envelope, and then again increases to the free stream value of V_∞ .

Fig. 6 shows the external air pressure distribution around the envelope, caused by this air flow.

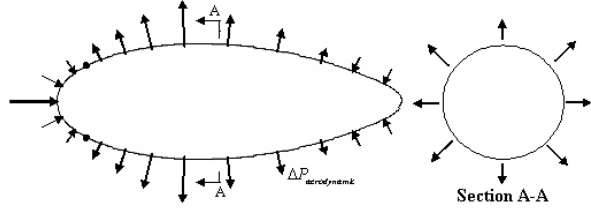


Fig. 6 Variation of pressure outside the envelope

If the internal pressure in the envelope is not sufficient, the nose will cave in under this external pressure. Thus internal static pressure at the nose w.r.t. atmosphere should be at least equal to the external stagnation pressure as calculated in Eq. (6)

$$\Delta P_{int} = \frac{1}{2} \rho V_\infty^2 \quad (6)$$

In practice, the differential pressure at the centerline is kept at 15% higher than the maximum anticipated internal static pressure. If the envelope is filled till the pressure at nose equals to ΔP_{int} , the differential pressure will not be the same everywhere, because of small hydrostatic effect occurring due to the gas as well as the air outside the envelope. Thus at a height h below the centerline, the differential pressure is calculated using Eq. (7)

$$\Delta P = \Delta P_{int_n} + \rho_{he} gh - \rho_{air} gh \quad (7)$$

It is clear from Fig. 7. that maximum differential pressure occurs at the maximum diameter.

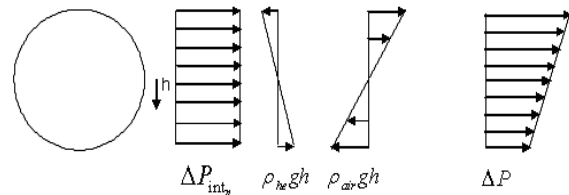


Fig 7. Pressure distribution due to various terms [5]

In order to get total differential pressure, we should add the aerodynamic suction pressure which is calculated using Eq. 8.

$$\Delta P_a = \Delta P_{aero} = \frac{1}{2} \rho V_\infty^2 C_p \quad (8)$$

The total differential pressure is given by Eq. 9.

$$\Delta P = \Delta P_{aero} + \Delta P_{int_n} + \rho_{he} gh - \rho_{air} gh \quad (9)$$

Once the differential pressure values have been calculated across different sections the maximum pressure coefficients can easily be identified from the pressure distribution plot as shown in Fig.7. The maximum value of Center of Pressure C_p occurs at the maximum diameter, and its magnitude is found to be -0.33. It may be noted that the maximum differential pressure occurring due to head also occurs at maximum diameter.

The total differential pressure at the maximum diameter is calculated using Eq. 10 as.

$$\Delta P_{max} = \Delta P_{aero,max} + \Delta P_{int_s} + (\rho_{air} - \rho_{he})g \frac{D}{2} \tag{10}$$

2.4 Envelope Material Selection

The selection of the appropriate material for the envelope is very crucial, to ensure adequate strength, durability, as well as low weight. Past studies [10] have shown that the weight of envelope material constitutes nearly 38% of empty weight of an airship, and 1% heavier material can result in ~ 2.5% loss in payload.

It is understandable that such diverse requirements viz., high load bearing capacity, low gas permeability and lower susceptibility to weather conditions cannot be met by a single material. Hence layers of different materials are joined together to form the envelope material [5]. Typical construction of envelope material is shown in Fig. 8.

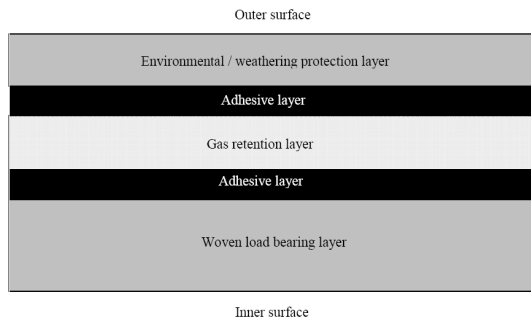


Fig. 8. Typical Construction of Envelope Material [5]

A qualitative comparison of the properties of various fabrics that are used for load bearing that were studied in order to meet the design requirements of airships is listed in Table 3.

Table 3. Qualitative comparison of properties & features of load bearing material

Property	C	PN	PD	PK
Dry Strength	G	E	E	E
Wet Strength	G	E	E	E
Ease in Bonding	E	G	F	F
Abrasion Resistance	F	G	G	E
Flammability	P	F	F	E
Flexibility	E	E	E	P
UV Resistance	F	F	G	P
Thermal Resistance	P	F	G	E

Note: C = Cotton, PN = Polyamide (Nylon) , PD = Polyester (Dacron), PK = Para-amid (Kevlar) G = Good, E= Excellent, F = Fair, P = Poor

It can be seen that Cotton is not used due to poor flammability, and fair abrasion resistance. Kevlar is not preferred due to poor flexibility and UV resistance, and also the high cost. Thus nylon and polyester are the two main candidates for choice of load bearing material, with nylon having lower cost and better bonding, while polyester has better flexibility and UV resistance.

Table 4 lists a comparison of few properties of these two fabrics.

Table 4. Comparison between properties of Nylon and Polyester

Property	Nylon	Polyester
Specific weight (g/m ²)	114	139
Tensile strength (GPa)	0.8	1.0
Strength to weight ratio	0.70	0.72
Weight gain due to hydrolysis	4%	Nil

Typical weight breakup of the various layers of fabric in an airship envelope material is shown in Table 5. It can be seen from Table 5 that load bearing material consists only about 43% of the total material weight. Thus use of nylon (which is 6.5 % heavier than polyester) as a load bearing material results in 2.8% additional envelope weight, thus resulting in about 7% loss

in payload. However, nylon is much less expensive compared to polyester, hence it is commonly used.

Table 5. Typical weight breakdown of various layers of an airship envelope fabric

Layer	Specific Weight (g/m ²)	%
Environmental Coating	92	39
Load Bearing	100	43
Gas retention	42	18
Total	234	100
Variation	±20	±8

For the *Micro* and *Mini* airships, special coated PVC fabric was used, keeping in mind the weight, cost and availability constraints. The properties of this material are listed in Table 6.

Table 6. Properties of envelope material for *Micro* and *Mini* airships

Property	Value	Units
H ₂ Permeability @ 25 cm H ₂ O column	3.75	liters/m ² /day
Break Strength along warp direction	1.68	kg/cm
Break Strength along weft direction	1.76	kg/cm
Specific Weight	141.1	g/m ²

2.5 Stabilizer Design

Selection of the geometry and size of stabilizers and fins of LTA vehicles requires a detailed stability and control analysis. This can be quite cumbersome, since the design data and knowledge about airships is not as easily available as that for fixed wing aircraft. In the absence of a readily available methodology, sizing of stabilizers and fins can be carried out by scaling down the dimensions of the stabilizer and fins of existing airships.

However, care must be taken to ensure that the scaling is done using data of airships which have envelopes of similar shapes and l/d ratios. One such methodology is highlighted in [1], in which a few non-dimensional parameters were identified and their average numbers were determined by studying the stabilizer and fin geometry of 15 existing airships.

For the *Micro* and *Mini* airship, the stabilizer and fin dimensions were scaled down

those of the PADD Demo and PaxCargo airships, respectively, since there were aimed to be the scaled prototypes of the same.

A schematic view of the stabilizer for *Micro* airship is shown in Fig 10. The relevant dimensions of the same are tabulated in Table 7.

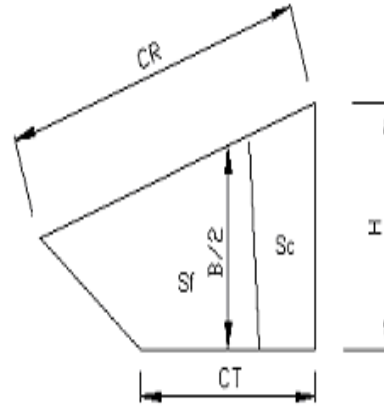


Fig. 10 Schematic view of a stabilizer

Table 7. Dimensions of Stabilizer and Fin of *Micro* airship

Parameter	Stabilizer	Fin
Surface area (m ²)	0.24	0.08
Tip chord (m)	0.54	0.17
Root chord (m)	0.91	0.19
Height (m)	0.54	
Semi-span (m)	0.43	

Many layouts are possible for airships such as “X”, “Y”, “inverted Y” or “+”. Of these, the “+” configuration is most commonly preferred for airships, since it results in a simple and effective control system [5], and hence was used for the *Micro* and *Mini* airships.

2.5 Propulsion System

Power plant is of prime concern in the engineering design of a Non-Rigid airship. Such airships usually operate with a gondola-mounted ducted propulsive system. A detailed overview of the power plant system, design issues in engine sizing and selection, advances in engine technology, various concepts for thrust vectoring and a methodology for sizing and selection of design features of an airship engine

have been outlined by the authors in a previous paper [11], so they are not being repeated here.

For the *Micro* airship, as mentioned earlier, an existing IC engine popularly used by aeromodelers was used, which is shown in Fig. 9.



Fig. 9 Engine used for the *Micro* Airship

The specifications of this engine are listed in Table 8. A similar engine (albeit with much higher power output) was used for the *Mini* airship.

Table 8. Specs. of the engine used for *Micro* airship

Type	0.15 LA-S (OSMG1415)
Displacement	2.49 cc
Bore	15.2 mm
Stroke	13.7 mm
RPM	2500 to 18000
Power output	0.41 BHP @ 17000 rpm
Weight	129.5 gm

2.6 Gondola Design

The gondola was sized to accommodate the receiver, battery package, fuel tank, engine and payload. The gondola shape was chosen to be a rectangular framework for ease in construction as described later.

2.7 Mooring Mast Design

A mooring mast is required for anchoring the airship to the base during payload assembly and integration. A non-guyed telescopic mooring mast was designed for *Micro* and *Mini*

airships. It consists of three telescopic modules made of standard aluminum sections, mounted on a tripod base with castor wheels for mobility, as shown in Fig. 11.

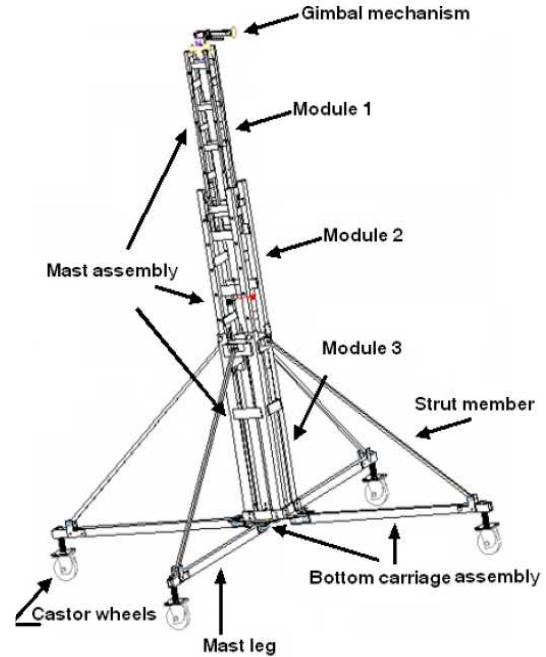


Fig. 11 Schematic design of mooring mast

The unique feature of this mast is that it has a gimballed mounting unit that allows the airship to freely weathercock while being attached. A drag measuring device is also incorporated in the gimbal mechanism that acts as an alerting system when the air loads exceed safe limit, as shown in Fig. 12.

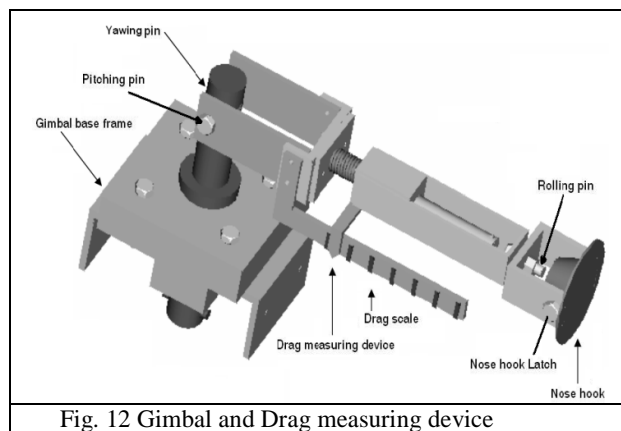


Fig. 12 Gimbal and Drag measuring device

The various modules and components of the mast were designed to enable quick assembly and transportation in a box that can be stowed

below a railway sleeper berth. The user-specified requirements and the structural considerations that affected the design of the mast are elaborated in a previous paper [12].

3 Fabrication of Sub Systems

This section outlines the various issues related to fabrication of the sub-systems of RC airships, with special reference to *Micro* airship.

3.1 Envelope fabrication

The co-ordinates of the GNVR shape were scaled down to match the *Micro* airship's length. A fourth order polynomial fit was generated using these co-ordinates, and the cross-sectional shape of the envelope was generated. It was decided to manufacture the envelope in four petals for ease and accuracy in fabrication, as well as to *Minimize* the wastage of the fabric. Production drawings for the envelope were generated on a vinyl banner which was later used as a master petal template containing the location and orientation markings of all external attachment viz., hooks for nose rings, nose batten, guy ropes, riggings and finger patches for confluence lines. The co-ordinates of the petals were generated along the length, and transferred to the envelope material. Fig. 13 shows the petal that was generated for the fabrication of the envelope for *Micro* airship.

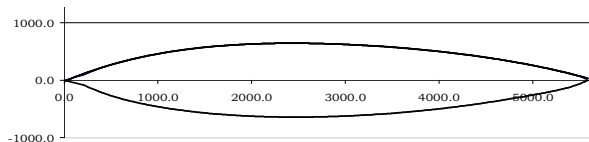


Fig. 13 Details of the petal of the *Micro* airship envelope

The various petals were joined to each other using the Radio Frequency (RF) sealing technique, in which heat energy generated from high frequency waves is used to melt the inner layers of the fabric, which act as a resistance in the circuit. On melting, the fabric layers fuse completely and an air tight sealing occurs. An RF sealing machine was used for fabrication, as shown in Fig. 14.



Fig. 14 Snap shot of envelope fabrication process

3.2 Gondola

The gondola is basically a box type structure made up of Balsa wood. To attach the gondola at the specified location on the envelope and also to support it, an aluminum frame was used with a curved top portion such that it exactly matched with the envelope contour. As shown in Fig. 15, a thick layer of sponge was provided on the curved portion to avoid piercing of the aluminum frame onto the envelope material. A three legged landing gear was mounted at bottom of gondola to support the airship during landing.

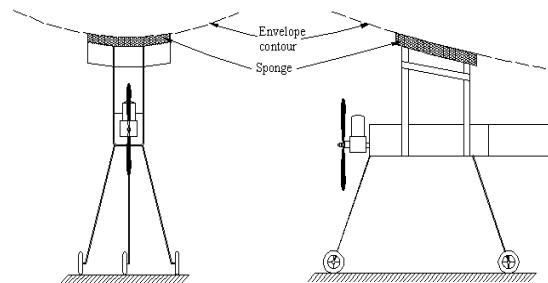


Fig.15 Sketch of the *Micro* airship gondola

3.3 Stabilizer

The fabrication of stabilizer was done using flat sheet of high density Thermocole (expanded polystyrene). Balsa wood was attached at edges to impart stiffness, and avoid local damage to the Thermocole due to impact loads.

Servo controllers were fitted to each fin in such a way that all control surfaces were made free to rotate 300 about the hinge line. These



Fig. 16 First Field Trial testing

Servos were provided with boosters for strengthening the signals coming from receiver.

In order to attach the stabilizer surfaces, a Velcro sheet 660 mm in length and 20 mm in width was pasted on the envelope. This was done by sticking the Velcro to a PVC patch, which in turn was joined to the envelope by means of RF heating.

Eight hooks were provided on the envelope surface (in two rows for four each) for attaching high strength wires, which were attached to the stabilizers. For each wire, one adjustable plastic screw was tied so as to maintain the required tension and rigidity of stabilizer with respect to the envelope.

4 Flight Testing and Operation

Several successful flight trials and demonstrations of the *Micro* and *Mini* airship were carried out by the PADD team. This section deals describes some key observations and results of these trials.

4.1 Operational Issues

Some of the major concerns dealt with before the flight testing were transportation and leak testing of the envelope. Use of non-rigid envelope and sub-assemblies that could be easily dismantled enabled the various system components be packed in cardboard cartons and transported to the required site for operation.

The other concern dealt with the leakage of gas due to small slits in the envelope that might occur during transportation. A complete manual check of the air filled envelope was carried out



Fig.17 Pre Flight check before second field trial

to seal off any possibilities of gas leaks. Following the gas leak testing was the complete integration of all to the sub assemblies and the inflation of the envelope. In order to fill the envelope with Helium, two cylinders, each of 7 m³ capacity at 140 kg/cm² were procured. The envelope was filled with helium directly from cylinder by controlling the valve on the cylinder. During filling it was observed that the PVC conduit at the rear end of the airship, which was connected to the helium cylinder, became very cold and hard. This was due to sudden expansion of Helium, resulting in very low temperature. It was observed that the additional ballast weight had to be added to the gondola in order to attain stability.

4.2 Flight Testing Results

The purpose of first flight was to check whether the airship could fly without stabilizers and also to check whether the engine selected was sufficient to meet the requirements. It was observed that envelope-gondola combination was unstable. The maximum speed achieved was estimated to be around 7 m/s. Photographs of the envelope in the first trial, and pre-flight checks being conducted on *Micro* airship are shown in Figure 16 and 17, respectively.

Based on these inferences the second flight test was conducted where in the flight duration was over two hours. The airship was flown at an altitude of up to 60 m above ground Level. The response of the control system was found to be very positive and effective even at low cruising speeds. The airship was steered in all directions in order to check its maneuvering capabilities.



Fig. 18 Micro airship just after takeoff



Fig. 19 Mini airship in flight

It was further noted that the angle of attack generated was far more than required thus leading to generation of unnecessary lift. This problem was encountered during the third field trial where in the gondola was repositioned in order to maintain dynamic stability.

During one of the field trials, a GPS was placed in the gondola, and was used to record flight parameters such as the altitude, speed, flight duration, track etc. Successful test results were obtained and the GPS readings recorded during the flight have been tabulated in Table 9.

Table 9: GPS recording for the third test flight

Total trip	1.9 km
Flight duration	10:12 min
Max. Speed	24.5 kmph
Avg. Speed	11.2 kmph
Max. Altitude	75 m
Cruising altitude	69 m
Track	0.3 km

5 Conclusions

The methodology for design of RC airship was found to be very useful in generating the preliminary design of the airship. It not only covers the basic aspects of airship design but also governs the various options that can be utilized depending on the user constraints. The fabrication module guided the team through the manufacturing and testing of the experimental prototypes of the airship that were flown as a part of the ongoing research. However, there still lies a tremendous scope for improving the current design from the aerodynamic point of view. Also further work is required for realization of fabrication of large airships. The study of the manufacturing requirements and costing for large airships needs to be undertaken separately. The operational issues have been dealt with, taking into consideration the human resource scenario in Southern Asia.

6 Acknowledgements

The methodology reported in this paper was developed while carrying out a consultancy project on Airship Design and Development for transportation of goods and passengers. The author would like to thank TIFAC (Technology Information Forecasting and Assessment Council), Department of Science & Technology of Government of India for sponsoring this study.

References

- [1] Pant, R., "A methodology for determination of baseline specifications of a non-rigid airship", Proceedings of AIAA's 3rd Aviation Technology, Integration, and Operations (ATIO) Technical Forum, November 2003, Denver, Colorado, USA.
- [2] Program on Airship Design & Development, <http://www.aero.iitb.ac.in/~airships>.
- [3] Vijay Ram, C., and Pant, R.S., "Multi-Disciplinary Shape optimization of Aerostat Envelope", Proceedings of AIAA's 7th Aviation Technology, Integration, and Operations (ATIO) Conference and 15th Lighter-Than-Air Systems Technology Conference, September 2007, Belfast, Northern Ireland, UK.

- [4] Kirilin, A. N., Ivchenko, B.A., report on “*Basic Design Parameters of Non-Rigid Airships*”, Russian Dirigible Society, Moscow, 2000.
- [5] Khoury G. A., Gillet J. D., Eds., “*Airship Technology*” Cambridge Aerospace Series: 10, ISBN 0 521 430 737, Cambridge University Press, 1999.
- [6] Narayana C.L., and Srilatha, K. R., “*Analysis of aerostat configurations by panel methods*”, NAL PD CF 0010, Technical Report, National Aerospace Laboratories, Bangalore, India, July 2000.
- [7] Lutz, T., Schweyher, H., Wagner S., “*Shape Optimization of Axi-symmetric Bodies in Incompressible Flow*”, Journal of Aircraft, Vol. 20, Feb. 1985, pp.520-526
- [8] Rao, GNV, “*Note on Optimization of the body of tethered aerostat airship*”, Unpublished paper, Indian Institute of Science Bangalore, 2006.
- [9] Thiele, J.R. “*Patterning Techniques for Inflatable LTA Vehicle*”, AIAA, *16th Fluid and Plasma Dynamics Conference*, Danvers, MA, July 12-14, 1983.
- [10] Pant, R., “*Conceptual Design Phase Study Report of Program on Airship Design and Development*”, Department of Aerospace Engineering, Indian Institute of Technology Bombay, May 2002.
- [11] Gawale, A, and Pant, R., “*Design Studies of a Powerplant System of Non-Rigid Airship*”, Proceedings of the *5th International Convention of The Airship Association*, Oxford, England, UK, August 2004.
- [12] Kale, S., and Pant. R., *Structural Design of Mooring Mast for Remotely Controlled Airship*, Proceedings of the *5th International Convention of The Airship Association*, Oxford, England, UK, August 2004.

Copyright Statement

The authors confirm that they, and/or their company or institution, hold copyright on all of the original material included in their paper. They also confirm they have obtained permission, from the copyright holder of any third party material included in their paper, to publish it as part of their paper. The authors grant full permission for the publication and distribution of their paper as part of the ICAS2008 proceedings or as individual off-prints from the proceedings.